

Investigation of Locally Resolved SOFC Characteristics along the Flow Path

P. Metzger, K. Friedrich, G. Schiller, E. Guelzow, H. Müller-Steinhagen
Deutsches Zentrum für Luft- und Raumfahrt e.V., Stuttgart, Germany

Introduction

Although tremendous progress in the last years has resulted in high power densities and the ability to use hydrocarbons as a fuel, solid oxide fuel cells still remain less developed than other fuel cell types [1]. The difference in maturity is mainly related to the need to investigate and understand SOFC processes under technically relevant operating conditions, namely high fuel utilization and the associated inhomogeneous current density and temperature distributions. Under these exacerbated operating conditions, durability of cells and stacks is reduced and degradation mechanisms are significantly distinct compared to idealized operation. Due to the electrochemical reaction, gradients of the reactant and product composition can be observed along the flow path of the gases. Especially high fuel utilization leads to a depletion of the fuel along the flow path and to varying power densities. Furthermore, the electrochemical reaction is associated with heat production, resulting in temperature gradients in such a system.

To optimize cells for operation in highly efficient systems a new measurement system is needed that allows the determination of local effects and the identification of critical operation parameters. Segmented cell components for measuring distribution of temperature and current density have been used successfully in polymer electrolyte fuel cells (PEFC) [2-4]. Recently, a similar approach has been used for the investigation of SOFC. However, the experimental challenges are higher in the case of high-temperature fuel cells since all segments have to be contacted reliably and homogeneously at 800 °C [5-6]. Nevertheless, the spatial resolution that is incorporated in the developed system allows the identification of possible steep gradients along the flow path. As a result this measuring tool represents an important methodological addition for the optimization of fuel cell operation and for the optimization of stack and cell designs.

Experimental Details

The present measuring system at DLR allows the characterization of SOFCs at 16 distinct measuring points along the flow path of the gases in the cell allowing to determine concentration gradients of reactants and products. These concentration gradients cause different electrochemical potentials at the SOFC electrodes and varying corrosion conditions which is especially important for metal-supported SOFC (MSC). With the measuring system that has been built up, current, voltage, temperature and impedance data as well as their distribution can be measured. Additionally 16 capillaries are integrated to take gas samples of the anode gas atmosphere to be analyzed. With this measuring tool the limiting components and/or processes in the system can be identified more easily. Square-shaped cells with a size of 100 cm² were integrated in metallic housings and sealed with glass sealing provided by the Fraunhofer Institute for Ceramic Technologies and Sintered Materials (IKTS) in Dresden. The metallic housing is subdivided into 16 galvanically isolated segments on both sides resulting in an active area of 73.96 cm². Variations in the contact resistances of the segments have to be taken into account in order to derive the reliable voltage-current density relationships. The procedure to analyse the measuring system has been reported before [6]. Recently, additional auxiliary voltage probes were integrated in the middle of 4 of the 16 segments along the flow path at the cathode side. These voltage probes were isolated from the metallic segments and are in direct contact with the cathode surface, allowing measurement of the overvoltages related to the contact resistance.

Fig. 1 shows the schematic layout of the set-up for the measurement system with segmented cells. Insulation material at the outer edges of the segments prevents the contact to the common metallic housing, and also the wires for current flux and voltage measurement are

isolated from the common plate. In addition, thermocouples are placed in the metallic segments to obtain the temperature distribution at different gas flow rates and also to correlate experimental data of the impedance measurement with the local temperatures. The common plate ensures a uniform contact pressure over all segments. The capillaries that are used to take gas samples from the anode gas atmosphere are not illustrated in the schematic representation.

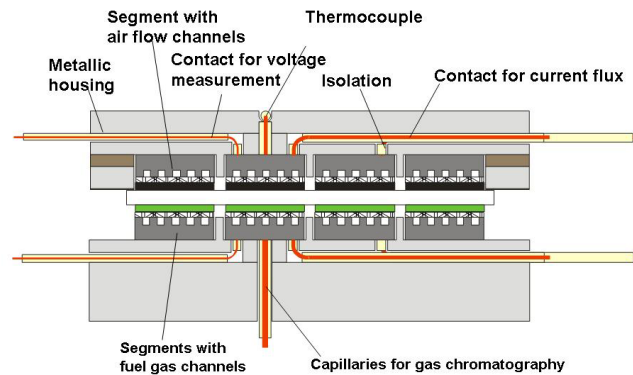


Figure 1. Schematic representation of the segmented cell approach of DLR for SOFC with both cathode and anode segmentation.

The method is quite flexible with regard to the integration of different cell designs. The following main cell concepts were investigated successfully: First, the investigation of the DLR concept of a planar SOFC based on advanced plasma deposition manufacturing is presented. This concept with consecutive deposition of all layers of a thin-film cell onto a porous metallic substrate support has been described in detail previously [7]. It is an alternative approach to standard SOFC manufacturing techniques which are based on wet powder processing and sintering methods. The MSC exhibits the advantage that only thin ceramic layers are needed. Therefore the mechanical properties are dominated by the metallic support leading to advantages in the mechanical integrity and the redox stability of the cell. In the segmented arrangement of metal-supported cells (MSC), only the cathode is segmented. In contrast, an electrolyte-supported cell (ESC2) is subdivided on the anode and cathode side. The third cell design that was investigated is an anode-supported cell (ASC2), which is also only sectioned on the cathode side for stability reasons. Both ESC2 and ASC2 were obtained from InDEC, the Netherlands. For the metal-supported cell a FeCrAlY substrate from Technetics, Florida, USA, was used. The plasma-sprayed coatings were NiO with YSZ for the anode, $ZrO_2 - 7 \text{ mol\% } Y_2O_3$ for the electrolyte and lanthanum strontium manganite (LSM) as cathode material. The ESC2 cell consists of a $45 \mu\text{m}$ thick nickel oxide/ gadolinia doped ceria (NiO / GDC) anode, a $90 \mu\text{m}$ thick yttria-stabilised zirconia (3 mol.%) (TZ3Y) electrolyte and a $40 \mu\text{m}$ thick LSM cathode. The ASC2 cell consists of a standard $540 \mu\text{m}$ thick NiO / YSZ anode with thin anode functional layer, a $7 \mu\text{m}$ thick yttria-stabilised zirconia (8YSZ) electrolyte and a $7 \mu\text{m}$ thick yttria doped ceria (YDC) layer to prevent chemical interaction with the adjacent $30 \mu\text{m}$ thick lanthanum strontium cobaltite ferrite (LSCF) cathode. For the contact of the electrodes, nickel and platinum meshes were inserted. The measuring system allows the determination of the $U(i)$ characteristics, impedance and temperature data over the complete cell and at the 16 distinct segments. To determine the balance of the anode gases, capillary tubes were integrated at the anode side at 16 measurement points that correspond to the cathodic segments. The sample gas composition was determined by gas chromatography. For details of the measuring system the reader should refer to [5].

Results and Discussion

As an example for the capability of this new analytical tool the power density distribution of the 16 segments, each 4.6 cm^2 wide, of an electrolyte-supported cell (ESC2) ($100 \times 100 \text{ mm}^2$) is shown in Fig. 2 at $800 \text{ }^\circ\text{C}$. The gas flow rates are $25.5 \text{ sccm/cm}^2 \text{ H}_2$ and $25.5 \text{ sccm/cm}^2 \text{ N}_2$ as

fuel, and 160 sccm/cm² air as oxidant. The fuel and air supply was performed in cross-flow configurations with the fuel inlet at segments 4,8,12,16 and air inlet at segments 1,5,9,13.

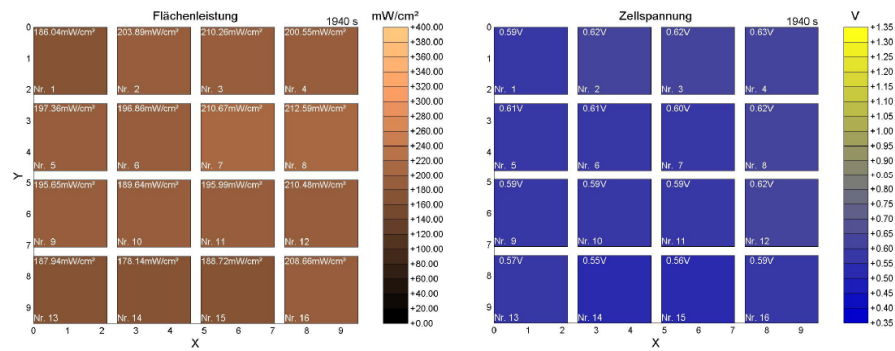


Figure 2. Power density distribution (left) and voltage distribution (right) of an electrolyte-supported cell at 800 °C.

The power density distribution varies somewhat over the cell. Maximum differences of about 34 mW/cm² at an average power density of 198 mW/cm² may be identified in Fig. 2. Also the voltages vary moderately from 0.55 to 0.62 V. There is also a slight increase of the power density of about 8-9 % in average over all segments from fuel inlet to fuel outlet. The main effect may be attributed to the inhomogeneous gas distribution at the inlet and to the sealing. It could be seen by local impedance spectroscopy that the current distribution is in good accordance with the local resistances. However, if the H₂ flow is reduced by a factor of 10 increasing the fuel utilisation dramatically a stable operation condition is an average power density of just 62 mW/cm² at 0.6 V and maximum difference of 56 mW/cm² between the highest and lowest segment. This demonstrates impressively the importance of operation conditions.

The influence of the variation of the hydrogen content on the performance of the cell can be seen in figure 3 in which measurements with an electrolyte-supported cell (ESC2) are shown. The content of hydrogen in the fuel gas supplied to an ESC2 cell was varied between 2 and 100 % (the supplementary gas was N₂). The power density distribution remains homogeneous when the system is operated at low fuel utilization ($f_{H_2} < 25\%$). With higher fuel utilization, significant gradients in the power density could be observed, resulting from both the variation of current density and voltage along the flow channels. At a hydrogen level of 10 % the fuel utilization already reaches nearly 80 % at the fuel outlet. Although the fuel utilization is already high the differences in the power densities vary only by about 20 %, i.e. from 149.5 to 184.3 mW/cm². With even lower hydrogen content the fuel utilization which is calculated from the average current density of the segments reaches levels of nearly 100 % or even above 100 %. Utilizations above 100 % are an artefact of the assumption that the gas distribution between the 4x4 matrix of the 16 segments is homogeneous. It is assumed that every segment line is fed with the same amount of gas, resulting in an identical residence time. In reality the current density distributions imply that the middle segment lines are supplied with a higher amount of gas. Since the inhomogeneous gas distribution can not be determined experimentally, this systematic error is present in all the measurements. It affects all concentration values similarly and therefore does not influence trends and the comparison of results.

To emphasize the influence of the inhomogeneous current density distribution it should be noted that at 2 % hydrogen content, segment 8 at the fuel exit contributes very little to the overall power density and only reaches a value of 8.8 mW/cm² compared to 87.1 mW/cm² at segment 5. The differences in the power density at higher hydrogen contents (20 % or more) are about 10 % or less and therefore hardly noticeable.

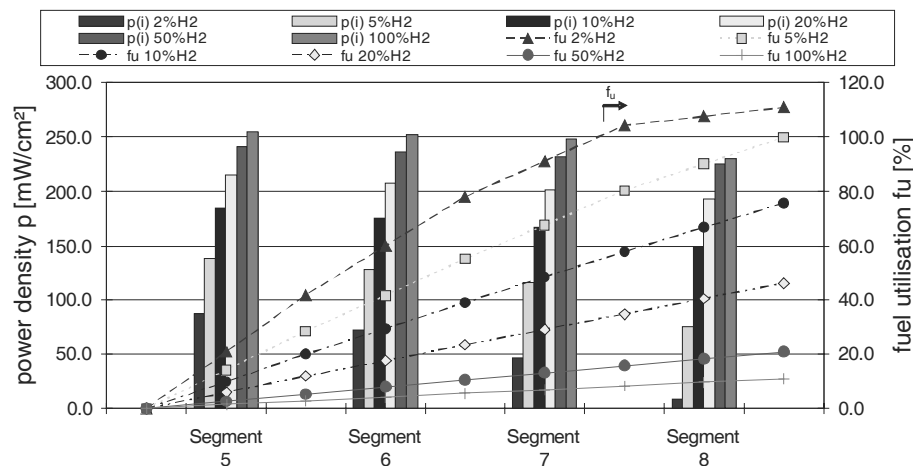


Figure 3. Locally resolved power density distribution (filled bars) and fuel utilization (filled symbols) for different hydrogen concentrations of the electrolyte supported cell ESC2 (INDEC).

Conclusions

Three main cell concepts were investigated successfully with the segmented cell method and strong variations of power density, fuel utilization and temperature were observed along the fuel path. The homogeneity of power density and of voltage along the flow path mainly depends on fuel utilization. At low hydrogen contents, anode re-oxidation conditions may be established which could be dangerous for long-term operation of the cells. Comparison of calculated hydrogen concentration with values measured by gas chromatography for a segment row shows acceptable agreement. The exemplary results show the importance and the usefulness of spatially resolved measurement of SOFC. In particular the operation of SOFC with hydrocarbon-derived fuel at high fuel utilization requires the application of this methodology to optimize performance and minimize degradation effects.

References

1. V.V. Krishnan et al, *Solid State Ionics*, **166** (1-2), 191 (2004).
2. C. Wieser, A. Helmbold, W. Schnurnberger, in *International Symposium on Proton Conducting Fuel Cells*, PV 98, p.457, The Electrochemical Society Proceedings Series, Pennigton, NJ (1998).
3. C. Wieser, A. Helmbold, E. Gülzow, *J. Applied Electrochemistry*, **30**, 803 (2000).
4. D.J.L. Brett et al., *Electrochemistry Communications*, **3**, 628 (2001).
5. P. Metzger, et al., in *Sixth European SOFC Forum Proceedings*, M. Mogensen, Editor, V 2, p. 867, European Fuel Cell Forum, Oberrohrdorf, Switzerland (2004)
6. P. Metzger, K.A. Friedrich, H. Müller-Steinhagen, G. Schiller, *Solid State Ionics*, **177**, 2045 (2006).
7. G. Schiller, R. Henne, M. Lang, R. Ruckdäschel, S. Schaper, *Fuel Cells Bulletin*, **21**, 7 (2004).